Membrane topology of the sodium ion-dependent citrate carrier of Klebsiella pneumoniae - Evidence for a new structural class of secondary transporters

Geest, Marleen van; Lolkema, Julius

Link to publication in University of Groningen/UMCG research database

Membrane Topology of the Sodium Ion-dependent Citrate Carrier of *Klebsiella pneumoniae*

EVIDENCE FOR A NEW STRUCTURAL CLASS OF SECONDARY TRANSPORTERS*

Marleen van Geest and Juke S. Lolkema‡

From the Department of Microbiology, Groningen Biotechnology and Biomolecular Sciences Institute, University of Groningen, 9751NN Haren, The Netherlands

The predicted secondary structure model of the sodium ion-dependent citrate carrier of *Klebsiella pneumoniae* (CitS) presents the 12-transmembrane helix motif observed for many secondary transporters. Biochemical evidence presented in this paper is *not* consistent with this model.

N-terminal and C-terminal fusions of CitS with the biotin acceptor domain of the oxaloacetate decarboxylase of *K. pneumoniae* catalyze citrate transport, showing the correct folding of the CitS part of the fusion proteins in the membrane. Proteolysis experiments with these fusion proteins revealed that the N terminus of CitS is located in the cytoplasm, while the C terminus faces the periplasm. The membrane topology was studied further by constructing a set of 20 different fusions of N-terminal fragments of the citrate transporter with the reporter enzyme alkaline phosphatase (CitS-PhoA fusions). Most fusion points were selected in hydrophilic areas flanking the putative transmembrane-spanning domains in CitS that are predicted from the hydropathy profile of the primary sequence. The alkaline phosphatase activities of cells expressing the CitS-PhoA fusions suggest that the polypeptide traverses the membrane nine times and that the C-terminal half of the protein is characterized by two large hydrophobic periplasmic loops and two large hydrophilic cytoplasmic loops.

CitS belongs to the family of the 2-hydroxycarboxylate transporters in which also the citrate carriers, CitPs, of lactic acid bacteria and the malate transporter, MleP, of *Lactococcus lactis* are found. Since the hydrophobicity profile of CitS is very similar to the hydrophobicity profiles of CitP and MleP, it is most likely that the new structural motif of nine transmembrane segments is shared within this new transporter family.

Bacterial secondary solute transporters use the free energy stored in electrochemical gradients of H^+ and/or Na^+ to drive the uptake of solutes by coupling the translocation of solute and cation(s) across the membrane. In *Klebsiella pneumoniae* a unique Na^+-dependent citrate carrier (CitS) is induced upon anaerobic growth on citrate (1). The gene coding for the transporter has been cloned and sequenced (2, 3), and the enzyme has been characterized and purified to homogeneity after expression in *Escherichia coli*. Studies with whole cells of *E. coli* expressing CitS and with membrane vesicles prepared from these cells have demonstrated that CitS obligatorily couples the translocation of the divalent citrate anion ($Hcit^{2-}$) to the translocation of two sodium ions and one proton (4, 5). More recent studies with purified CitS (6) reconstituted in proteoliposomes have raised some doubt about the electrogenic nature of the translocation catalyzed by the transporter, and it was concluded that one of the two Na^+ ions recycle during the translocation of citrate (7).

The *citS* gene encodes a highly hydrophobic protein with a predicted molecular mass of 47,531 Da. The gene is homologous to the genes coding for the citrate carriers of lactic acid bacteria, CitPs (8, 9), and the malate carrier of *Lactococcus lactis*, MleP.[1] The latter two transporters are not Na^+-dependent but, instead, translocate divalent citrate or malate in symport with a single proton. CitP and MleP translocate negative charge into the cell and are involved in secondary proton motive force generation (11–13). The family of the three transporters is termed the bacterial 2-hydroxycarboxylate transporters, since the physiological substrates are citrate, malate, and lactate.

The global secondary structure of bacterial secondary solute transporters is believed to be similar (*e.g.* see Ref. 14). The proteins are predicted to consist of 12 transmembrane segments (TMSs),[2] which traverse the membrane in an α-helical structure. The helices are connected by hydrophilic loops that are usually larger at the cytoplasmic side of the membrane than at the periplasmic side. The models are predicted from the hydropathy profile of the primary sequences in which the hydrophobic domains correspond to the TMSs. The orientation of the protein in the membrane is determined by the "positive inside rule" of von Heyne (15) and places both the N and C termini in the cytoplasm. For a number of secondary transporters like the lactose and melibiose transporters of *E. coli*, substantial evidence has been presented to support general features of the models (Refs. 16 and 17; for a general review see Ref. 18). Fig. 1 shows the secondary structure model for CitS predicted from the primary structure. The protein also folds in 12 TMSs, but in contrast to what is observed for many other secondary carriers, the C-terminal half is characterized by large periplasmic and short cytoplasmic loops. Also, in this part of the molecule, von Heynes "positive inside rule" is not very apparent (19). The hydropathy profile of the primary sequences is highly conserved in the 2-hydroxycarboxylate transporter family, and similar models are predicted for CitP and MleP (13).

---

[1] M. Bandell, V. Ansanay, N. Rachidi, S. Dequin, and J. S. Lolkema, submitted for publication.

[2] The abbreviations used are: TMS, transmembrane segment; BAD, biotin acceptor domain; RSO, right side-out; ISO, inside-out; XP, bromo-4-chloro-3-indolyl-phosphate (toluidine salt); PCR, polymerase chain reaction.

In this paper, we present biochemical evidence that is not consistent with the predicted secondary structure of CitS. Tagging of the N terminus and C terminus of CitS with the biotin acceptor domain (BAD) of the oxaloacetate decarboxylase of *K. pneumoniae* showed that the N and C termini are at the cytoplasmic and periplasmic face of the membrane, respectively, indicating that the protein traverses the membrane an odd number of times. Subsequent construction of fusion proteins consisting of N-terminal fragments of CitS and the reporter molecule alkaline phosphatase, PhoA (20), suggests that CitS contains nine transmembrane-spanning segments.

EXPERIMENTAL PROCEDURES
Bacterial Strains and Growth Conditions

E. coli strains JM109, BL21(DE3), and CJ236 were routinely grown in Luria broth medium at 37 °C. When appropriate, carbenicillin, chloramphenicol, and kanamycin were added at final concentrations of 100, 50, and 20 μg/ml, respectively. CitS derivatives were expressed in *E. coli* BL21(DE3) without induction with isopropyl 1-thio-β-D-galactopyranoside. For *in vivo* biotinylation of CitS-BAD fusion proteins, D-biotin was included in the medium at a final concentration of 1 μg/ml. Citrate transport activity was detected as blue colonies on Simmons citrate agar plates (Difco). Alkaline phosphatase activity was detected as blue colonies on LB agar plates containing 5-bromo-4-chloro-3-indolyl-phosphate (toluidine salt; XP) at a concentration of 40 μg/ml.

Genetic Manipulations

Recombinant DNA Techniques—Standard recombinant DNA procedures were used essentially as described by Sambrook *et al.* (21). The *citS* gene was cloned downstream of the T7 promoter on a pBlueScript phagemid (Stratagene) from which the Lac promoter region was deleted (see below). All genetic manipulations of the *citS* gene were performed in *E. coli* JM109, in which *citS* is not expressed. Expression of the genes was obtained in *E. coli* BL21(DE3), which contains a chromosomal copy of the gene coding for T7 polymerase (22). Site-directed mutants were constructed following the Kunkel method (23). Nucleotide sequencing was done using the dideoxy chain-terminating method (24) or with a Vistra 725 automated sequencer.

Construction of NcoI Mutants pSNxxx—The Lac promoter region was deleted from plasmid pBlueScript II SK by deletion mutagenesis. The mutagenic primer was complementary to sequences downstream and upstream of the promoter region. The nucleotide sequence of the primer was 5′-CAATTCCACACGCCTGGGGTGCC-3′. Successful deletion of the Lac promoter in the resulting vector pSKΔL followed from blue/white screening on 5-bromo-4-chloro-3-indoyl β-D-galactoside plates and subsequent restriction analysis. A *Hin*dIII/*Bam*HI fragment containing the *citS* gene was restricted from pKS*citS* (5) and ligated into pSKΔL restricted with the same two enzymes. In the resulting plasmid, pSKΔL*citS*, the *citS* gene was downstream of the T7 promoter on the pBlueScript vector. Unique *Nco*I restriction sites (CCATGG) were introduced throughout the *citS* gene in pSKΔL*citS* by site-directed mutagenesis. The mutagenic oligonucleotides are listed in Table I. The mutants were checked by restriction analysis and dideoxy sequencing of the region around the *Nco*I site. The resulting plasmids are designated pSNxxx in which xxx is the residue number of the methionine residue in the CitS mutants coded by the ATG codon in the *Nco*I site. The positions of the methionine residues are indicated by the *arrows* in Fig. 1.

Construction of BAD Fusion pSBxxx—Plasmid pTC57 containing the coding sequence for the BAD of the oxaloacetate decarboxylase of *K. pneumoniae* inserted in the *lacY* gene was a gift from H. R. Kaback and described in Ref. 25. The BAD sequence was amplified by PCR using a forward (5′-GGGGGGCGGACCATGGCTGCTCCTGCTCC-3′) and reverse (5′-CGCCCCTGCCATGGCCCGACCCTCGATCAGGGTCATCAGGGTGTC-3′) primer that introduced *Nco*I sites in the flanking regions. The ATG codons of the *Nco*I sites were in frame with the BAD sequence. The PCR fragment was digested by *Nco*I and ligated into the *Nco*I sites of pSN1 and pSN445 (Fig. 2*A*) The orientation of the insert was checked by restriction analysis using a unique *Nar*I site that is located asymmetrically in the BAD coding sequence. The resulting plasmids, pSB1 and pSB445, code for the BAD fused to the N and C termini of CitS, respectively.

Construction of PhoA Fusions pSAxxx—The *Hin*dIII/*Sac*I fragment of plasmid pPHO7 (26) containing an open reading frame coding for the mature part of alkaline phosphatase was cloned into the multiple cloning site of pSKΔL. The unique *Nco*I site in the *phoA* gene was destroyed

TABLE I
Oligonucleotides used for construction of NcoI sites in citS and citS-phoA fusions

Construct[a]	Oligonucleotide (5′–3′)	Predicted localization[b]
SN1	GGATAACGT**CC**A**TGG**CTAACATG	Cyt
SA46	ATCGGTGG**CC**A**TGG**CGTTATAAAAATGTGA	Per
SN72	ATTGGCAAGC**CC**A**TGG**CAATATTCAA	Cyt
SA103	GATAGCATC**CC**A**TGG**CTTTCTGCGTAAAAATACC	Per
SN141	CTGCTGAAAT**CC**A**TGG**TCGGCTATATT	Cyt
SN174	CCAGTGGATCGCA**CC**A**TGG**TGCTGTACGTC	Per
SN200	TACCACTC**CC**A**TGG**CCGGTCGTTCT	Cyt
SN239	ATCATCGGCAAAAAACACA**CC**A**TGG**TGAGCGGC	Per
SN260	GAAGATGAGA**CC**A**TGG**GACAAATC	Per
SN290	GCGAAGAAAA**CC**A**TGG**CCAGCATTGGC	Cyt
SA298	CGCGAAATAGT**CC**A**TGG**CCACACCGCCAATGCT	Mem
SN308	GGATGGTGCTGA**CC**A**TGG**CCGCGCTG	Per
SA319	TTTGATTT**CC**A**TGG**GAGCACAGCCCCGGAGGC	Per
SN328	GGTGCTAAAC**CC**A**TGG**CTGATTTCTTC	Per
SA344	GCAGACGC**CC**A**TGG**CGACCATCAGCACCCA	Mem
SN360	GCCATCACC**CC**A**TGG**CTAACGTT	Cyt
SA379	CCAGCCACC**CC**A**TGG**CCGCGCCGAGCACCGC	Mem
SN389	CTTCTTCCC**CC**A**TGG**GAATCGGCCATC	Per
SN399	GCAGGCCTGT**CC**A**TGG**CCAACCGCGGC	Per
SN427	GCGCAAATCT**CC**A**TGG**GTTTGGGCGGCGGT	Per
SN445	TGTTCGGCA**CC**A**TGG**TTTAACCCAT	Cyt

[a] The numbers correspond to the residue that is coded by the ATG codon in the *Nco*I site (underlined). Nucleotides in boldface type indicate mutations. Constructs indicated as SNxxx represent *Nco*I site mutants of *citS* constructed by site-directed mutagenesis. The oligonucleotide is the mutagenic primer. Constructs indicated as SAxxx represent *citS-phoA* fusions constructed by PCR. The oligonucleotide is the reverse primer, while the forward primer used was the mutagenic primer used to construct SN1 or SN174 (see "Experimental Procedures").

[b] Periplasmic (Per), cytoplasmic (Cyt), or membrane (Mem) localization of the methionine residue coded by the ATG codon according to the predicted model in Fig. 1.

by constructing a silent mutation by site-directed mutagenesis using the following mutagenic primer 5′-AACGTACCACGGCAATATC-3′. An *Nco*I site was engineered at the beginning of the open reading frame with the primer 5′-TGCAGGTCGACCATGGAGGATCCC-3′. The resulting plasmid is termed pSK*phoA*. The *Nco*I/*Sac*I fragment of pSK*phoA*, encoding mature PhoA, was ligated into plasmid pSNxxx digested with *Nco*I and *Sac*I (Fig. 2*B*). The resulting vectors encode mature alkaline phosphatase fused to the C terminus of N-terminal fragments of CitS of different lengths (CitS-PhoA fusions). The plasmids were designated pSAxxx, in which xxx indicates the fusion point.

The CitS-PhoA fusions indicated in Table I as SAxxx were constructed by the PCR technique. The coding region of the *citS* gene on pSN1 was replaced by the *phoA* gene by ligating the *Nco*I/*Sac*I fragment of pSK*phoA* into pSN1 digested with the same two enzymes, yielding pSKN*phoA*. Two N-terminal fragments of the *citS* gene, coding for residues 1–46 and residues 1–103, were amplified by PCR while *Nco*I sites were engineered around the start codon of *citS* and around residues 46 and 103, respectively. The obtained PCR products were ligated in the *Nco*I site of pSKN*phoA*, yielding pSA46 and pSA103. Plasmids pSA298, pSA319, pSA344, and pSA379 were constructed similarly by amplifying the appropriate fragments of *citS* and ligating the fragments in the *Nco*I site of mutant pSN174. All fusion sites and the inserted PCR fragments were sequenced using the Vistra 725 automated sequencer.

Biochemical Techniques

Alkaline Phosphatase Activity—Alkaline phosphatase activity of the cells was assayed by measuring the rate of *p*-nitrophenyl phosphate hydrolysis mainly as described by Michaelis *et al.* (27). After collection of the cells, they were resuspended in 1 M Tris-HCl, pH 8, and after incubation for 5 min at 37 °C the substrate *p*-nitrophenyl phosphate was added at a final concentration of 0.66 mg/ml. Activities were expressed in Miller units ($1000 \times A_{420}/A_{600}$/time). The activities were corrected for the background activity measured with *E. coli* BL21(DE3) cells harboring plasmid pSKΔL*citS*, which amounted to 5 Miller units for exponentially growing cells and 10 Miller units for overnight grown cells.

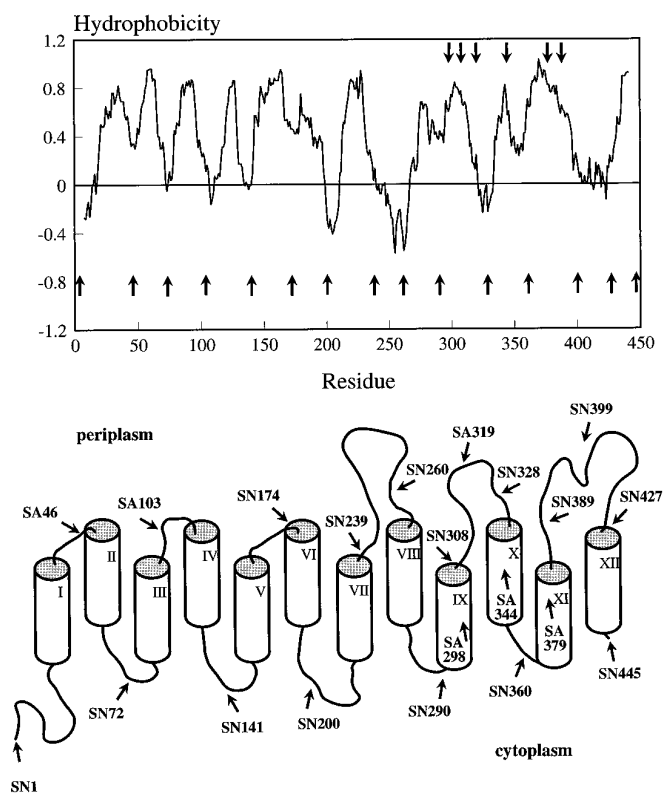*Immunoblot Analysis*—Cells were resuspended to an A_{600} of 10,

FIG. 1. **Hydropathy profile (*top*) and predicted secondary structure model of CitS (*bottom*).** A sliding window of 13 residues was used in the calculation of the profile to emphasize the hydrophilic regions. The secondary structure model was predicted from the hydropathy profile using the algorithm of Eisenberg (10). The *cylinders* indicate membrane-spanning segments. The lengths of the *connecting loops* are roughly according to the number of residues in the loops. *Arrows* indicate fusion sites in CitS-PhoA fusion proteins constructed by site-directed mutagenesis (SNxxx) or PCR (SAxxx).

diluted with one-third volume of loading buffer, and boiled for 3 min, after which 2.5-μl samples were loaded onto SDS-polyacrylamide gels containing 10 or 12.5% polyacrylamide. After running of the gels, the proteins were transferred to Immobilon-P membranes (Millipore) by semidry electrophoretic blotting. PhoA fusion proteins were detected with monoclonal antibodies directed against PhoA at a dilution of 1:5000, and biotinylated proteins were detected with Ap-labeled streptavidin also at a dilution of 1:5000. Antibodies and streptavidin were visualized using the Western-light™ chemiluminescence detection kit with CSPD™ as a substrate as recommended by the manufacturer (Tropix).

Preparation of Membranes and Spheroplasts—Cells were grown to an A_{600} of 1, harvested, and washed once with 50 mM KP$_i$, pH 7, 100 mM NaCl. Inside-out (ISO) membrane vesicles were prepared by passing the cell suspension through a French pressure cell operated at 20,000 p.s.i. Membranes were collected by ultracentrifugation for 45 min at $45,000 \times g$ in a Beckman Ti70 rotor. Right side-out (RSO) membrane vesicles were prepared by the osmotic shock lysis procedure (28). The membranes were stored in liquid nitrogen. Spheroplasts were prepared essentially as described by Herzlinger *et al.* (29). Cells from a 150-ml culture were resuspended in 7.5 ml of 10 mM Tris-HCl, pH 8, 0.75 M sucrose, and incubated at 20 °C for 10 min. After the addition of 20 μl of a 10 mg/ml lysozyme solution followed by additional incubation for another 10 min, the suspension was diluted 3-fold with a solution containing 1.5 mM K-EDTA and 10 mg/ml lysozyme. After incubation for 1 h, the spheroplasts were harvested by centrifugation for 3 min in a tabletop centrifuge (Eppendorf) and washed once in 100 mM potassium phosphate, pH 7, 0.5 M sucrose.

Proteinase K Treatment—RSO and ISO membranes were resuspended to a protein concentration of 0.2 mg/ml in a total volume of 100 μl. Proteinase K was added in a volume of 10 μl containing 100 mg/ml. The reaction was stopped by mixing an aliquot with a phenylmethylsulfonyl fluoride solution at a final concentration of 1 mg/ml. The experiment was performed on ice.

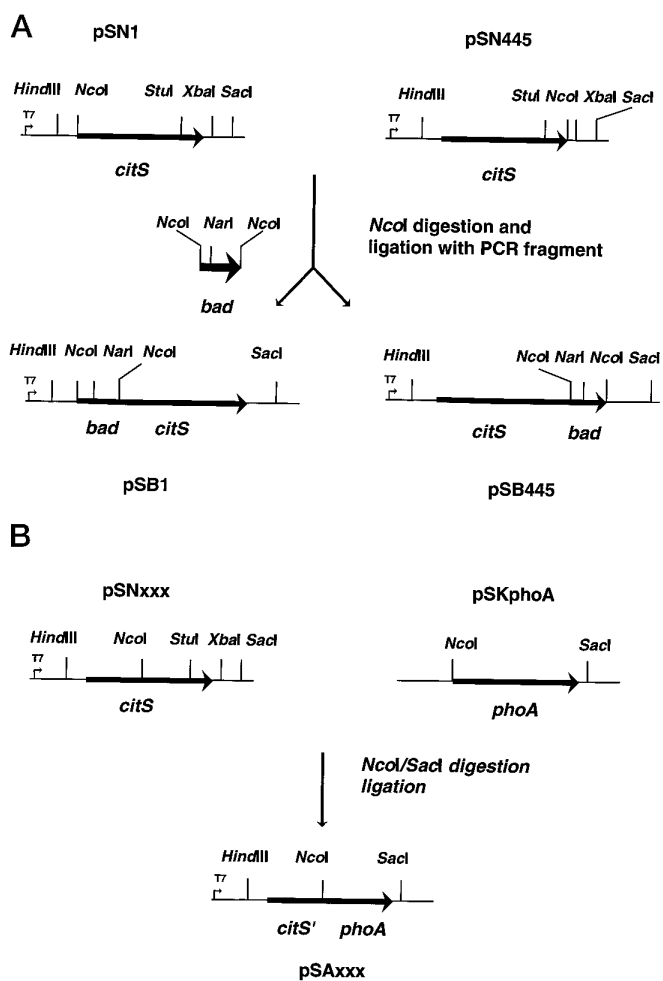*Transport Assays*—Citrate uptake in whole cells was measured by

FIG. 2. **Construction of pSBxxx (A) and pSAxxx plasmids (B).** The genes are indicated by *thick arrows*. The *NcoI* site in pSNxxx may be at any of the positions indicated by the *arrows* in Fig. 1. *citS'* denotes a 5' fragment of the *citS* gene.

the rapid filtration method as described by Lolkema *et al.* (5). Uptake was measured in 50 mM KP$_i$, pH 6, containing 5 μM [1,5-^{14}C]citrate at 30 °C.

Materials—[1,5-^{14}C]Citrate (110 mCi/mmol) was obtained from Amersham International (Buckinghamshire, UK), Alkaline phosphatase-labeled streptavidin from Boehringer Mannheim and the monoclonal antibodies against alkaline phosphatase from Chemicon International, Inc. (Temecula, CA). Oligonucleotides were obtained from EuroSequence (Groningen, The Netherlands).

RESULTS

Construction of CitS Fusion Proteins—To determine the cellular localization of the N and C termini of the Na$^+$-dependent citrate carrier of *K. pneumoniae* (CitS), gene fusions were constructed coding for the CitS protein fused with the BAD of the α-subunit of the oxaloacetate decarboxylase of *K. pneumoniae* at both the N and C termini and PhoA at the C terminus. Expression and *in vivo* biotinylation of the fusion proteins were analyzed by Western blotting of whole cell extracts using alkaline phosphatase-labeled streptavidin, which binds specifically to biotin, and a monoclonal antibody against alkaline phosphatase (Fig. 3). Detection with streptavidin resulted in a band with a molecular mass of 22 kDa observed in all lanes (Fig. 3A). This band corresponds to acetyl-CoA carboxylase of *E. coli*, which is the only known biotinylated protein in *E. coli*. Cells harboring plasmids pSB1 and pSB445 show an additional band not observed in the control cells with an apparent mass of 48 kDa (Fig. 3A, *lanes 2* and *3*), demonstrating that the CitS-BAD fusion proteins are synthesized, biotinylated *in vivo*, and fur-
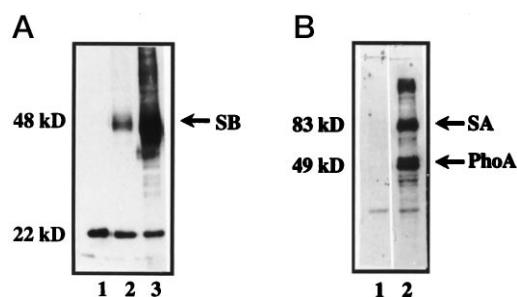
FIG. 3. **Western blot analysis of N- and C-terminal CitS fusion proteins.** Cells expressing CitS constructs were run on a 12.5% SDS-polyacrylamide gel and, after blotting, analyzed for biotinylated proteins (*A*) and alkaline phosphatase (*B*). *A* and *B*, *lane 1*, pSKΔL*citS*. *A*, *lane 2*, pSB445; *lane 3*, pSB1. *B*, *lane 2*, pSA445. The *arrows* labeled *SB*, *SA*, and *PhoA* indicate the CitS-BAD fusion protein, the CitS-PhoA fusion protein and mature PhoA, respectively.

TABLE II
Activities of the CitS fusion proteins

Initial rates of citrate uptake were measured in whole cells expressing wild type CitS, CitS fused with its N terminus (SB1) and C terminus (SB445) to the BAD of the oxaloacetate decarboxylase of *K. pneumoniae*, and CitS fused with its C terminus to the mature form of alkaline phosphatase (SA445).

Construct	Citrate uptake activity	Alkaline phosphatase activity
	nmol/min · mg protein	*Miller units*
CitS	4.7	5
SB1	2.5	
SB445	2.0	
SA445	3.0	484

thermore stable. The size of the fusion proteins was the same as observed before for a similar construct (6). The amount of biotinylated SB1 (*lane 3*) is much higher than the amount of biotinylated SB445 (*lane 2*). This is due to different levels of expression of the two fusion proteins and/or to a less effective *in vivo* biotinylation of SB445 (see below).

Growth of *E. coli* strain BL21(DE3) expressing wild type CitS in rich medium does not result in expression of chromosomally encoded alkaline phosphatase (Fig. 3*B*, *lane 1*). With cells expressing the CitS-PhoA fusion protein SA445 two major bands are observed (*lane 2*). The band at an apparent mass of 83 kDa corresponds to the fusion protein, and the band at 49 kDa corresponds to mature PhoA, which indicates that a considerable amount of the fusion protein is partially degraded. The additional band at higher molecular mass corresponds to the dimeric fusion protein.

Activity of the Fusion Proteins—Wild type *E. coli* cells exhibit a negative phenotype on Simmons agar indicator plates because they lack a citrate uptake system. Expression of wild type CitS results in citrate uptake and metabolism as evidenced by the appearance of blue colonies on the plates. Expression of the fusion proteins SB1, SB445, and SA445 all result in a positive phenotype, indicative of active citrate transport proteins. The citrate transport activity was examined in more detail by uptake experiments using whole cells. The initial citrate uptake rate of cells expressing the different fusion proteins was about half the rate observed with cells expressing wild type CitS (Table II). Since the expression level of wild type CitS is not known, specific activities cannot be given. The citrate uptake activities of SB1 and SB445 are similar, suggesting that the degree of biotin incorporation into the C-terminally fused BAD is low rather than that the expression of the proteins is very different. Although no solid conclusions can be made about the specific activity of the fusion proteins, the data show that the fusion proteins are active and, therefore, that the correct folding of CitS in the membrane is maintained.

Localization of N and C Termini—The cellular localization of the biotinylated N and C termini of SB1 and SB445 was studied by determining the susceptibility of the BAD to proteinase K digestion in ISO and RSO membrane vesicles. A complete loss of the BAD-CitS fusion protein within 10 min was observed when ISO membrane vesicles of cells expressing SB1 were treated with proteinase K, indicating that the BAD is fully accessible from the cytoplasmic side of the membrane (Fig. 4, *top*). In contrast, treatment of RSO membrane vesicles prepared from the same cells resulted in slow degradation of the SB1 band at 48 kDa with a concomitant increase of a band at 31 kDa and a less intense band at 29 kDa. The former was stable upon prolonged proteinase K treatment. In total, no loss of
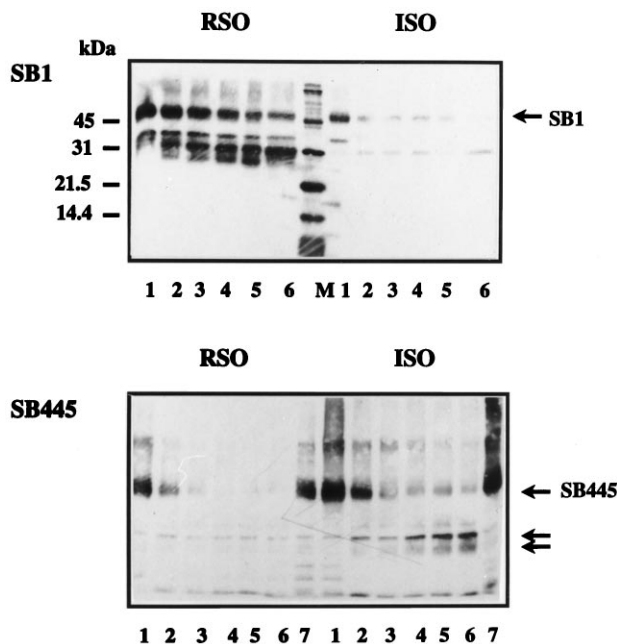

FIG. 4. **Proteinase K digestion of SB1 and SB445.** ISO and RSO membrane vesicles were prepared from *E. coli* BL21(DE3) cells expressing SB1 (*top*) and SB445 (*bottom*). Membranes were treated for 0, 5, 10, 15, 30, and 45 min (*lanes 1–6*, respectively) with proteinase K. Samples were loaded on a 10% (*A*) or 12.5% (*B*) SDS-polyacrylamide gel, and the biotinylated proteins were detected with alkaline phosphatase-labeled streptavidin. *Top*, *lane M*, biotinylated marker. *Bottom*, *lane 7*, as *lane 6* except that proteinase K was omitted in the procedure. The positions of the CitS-BAD fusion proteins and the resulting degradation products (*B*) are indicated by *arrows*.

signal intensity is observed, suggesting that the BAD itself is not accessible but that the CitS part of the fusion protein is cleaved in one or more periplasmic loops. These results show that the N terminus of CitS is located at the cytoplasmic face of the membrane. Surprisingly, the opposite result was obtained with ISO and RSO membrane vesicles isolated from cells expressing the C-terminal CitS-BAD fusion SB445. Proteinase K treatment of the RSO membranes resulted in complete and rapid loss of the fusion protein (Fig. 4, *bottom*), whereas treatment of the ISO membranes resulted in slower loss of the 48-kDa band and, at the same time, the appearance of two new bands at lower molecular weights, presumably as a result of cleavage of the CitS moiety in cytoplasmic loops. The total intensity of the bands in the ISO membranes is reduced, which may be caused by a different blotting efficiency of the fragments.

The periplasmic location of the C terminus is consistent with the alkaline phosphatase activity of the C-terminal PhoA fusion SA445. Alkaline phosphatase is only enzymatically active when it is translocated to the periplasm. The protein is synthesized as an inactive precursor in the cytoplasm and targeted
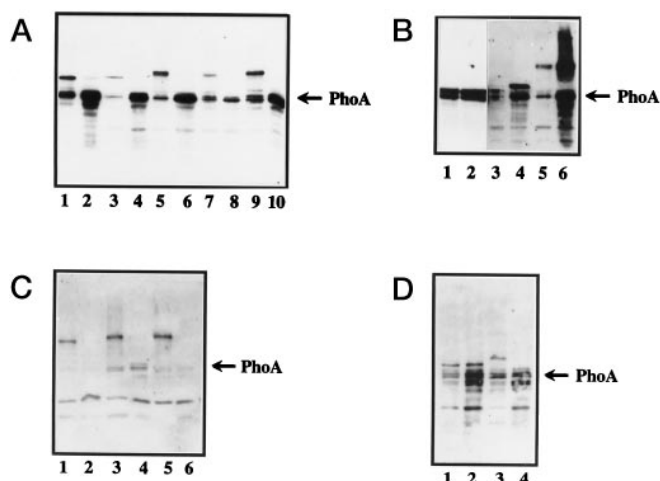
FIG. 5. **Western blot analysis of the CitS-PhoA fusion proteins.** Cells expressing fusion proteins with a blue (*A* and *B*) and white (*C* and *D*) phenotype on XP plates were run on a 12% SDS-polyacrylamide gel, and the fusion proteins were detected with a monoclonal antibody directed against PhoA. Cell samples were taken from exponentially growing cultures (*odd numbered lanes*) and from overnight cultures (*even numbered lanes*). *A*, SA174 (*lanes 1* and *2*), SA200 (*lanes 3* and *4*), SA290 (*lanes 5* and *6*), SA308 (*lanes 7* and *8*), SA328 (*lanes 9* and *10*). *B*, SA46 (*lanes 1* and *2*), SA103 (*lanes 3* and *4*), SA445 (*lanes 5* and *6*). *C*, SA260 (*lanes 1* and *2*), SA389 (*lanes 3* and *4*), SA399 (*lanes 5* and *6*). *D*, SA72 (*lanes 1* and *2*), SA141 (*lanes 3* and *4*). The *arrow* labeled *PhoA* indicates mature PhoA. The band with the higher molecular weights observed in the *odd numbered lanes* represents the full-length fusion proteins.

TABLE III
Properties of CitS-PhoA fusion proteins

Fusion protein	XP plates[a]	PhoA activity[b]		Localization[c]	
		Exponential	Stationary	PhoA fusions	Predicted
SA46	Blue	375	770	Per	Per
SA72	White	0	30	Cyt	Cyt
SA103	Blue	66	126	Per	Per
SA141	White	0	12	Cyt	Cyt
SA174	Blue	400	650	Per	Per
SA200	Blue	28	300	Per	Cyt
SA239	White	0	15	Cyt	Per
SA260	White	0	0	Cyt	Per
SA290	Blue	85	295	Per	Cyt
SA298	Blue	87	162	Per	Mem
SA308	Blue	33	73	Per	Per
SA319	Blue	86	583	Per	Per
SA328	Blue	100	450	Per	Per
SA344	Blue	72	176	Per	Mem
SA360	Blue	103	211	Per	Cyt
SA379	White	0	6	Cyt	Mem
SA389	White	1	8	Cyt	Per
SA399	White	0	8	Cyt	Per
SA427	White	1	2	Cyt	Per
SA445	Blue	171	680	Per	Cyt

[a] Isolates were plated on LB agar plates containing the chromogenic substrate XP for alkaline phosphatase (40 μg/ml).

[b] Alkaline phosphatase activity was measured of cells of exponential growing cultures, after which the same cultures were allowed to grow overnight and the activity was measured again.

[c] Periplasmic (Per), cytoplasmic (Cyt), or membrane (Mem) localization determined from the PhoA activities and the predicted model in Fig. 1.

to the periplasm by a signal sequence at the N terminus. Membrane proteins or fragments thereof with the C terminus in the periplasm can take over the function of the signal sequence, which is the basis of the frequently used *phoA* gene fusion technique to determine the topology of membrane proteins (20). The chromosomal copy of alkaline phosphatase is not expressed when *E. coli* BL21(DE3) is grown in rich medium (Fig. 3*B*, *lane 1*), and the cells appear as white colonies on alkaline phosphatase indicator plates containing the chromogenic substrate XP. In contrast, *E. coli* cells harboring pSA445 grow as blue colonies on XP plates, and their alkaline phosphatase activity is 2 orders of magnitude higher than observed for cells expressing wild type CitS (Table II). Together, these results show that the N terminus of CitS is located in the cytoplasm and that the C terminus is in the periplasm.

CitS-PhoA Fusion Proteins—The predicted secondary structure model (Fig. 1) of CitS derived from hydropathy profiling showed 12 TMSs, suggesting that the N and C termini of CitS are located at the same face of the membrane, which is at variance with the experimental data presented above. Another 19 different positions in CitS were selected for the construction of CitS-PhoA fusions. Most junctions were chosen in the hydrophilic stretches of the protein flanking the predicted TMSs (Fig. 1, *upward pointing arrows*).

The alkaline phosphatase activity of *E. coli* BL21(DE3) cells harboring the pSAxxx plasmids was determined by blue/white screening on XP plates and by measuring the alkaline phosphatase activity of cells harvested in the early exponential growth phase and in the stationary phase (Table III). The alkaline phosphatase activities of exponentially growing cells that grow as blue colonies on XP plates are at least 1 order of magnitude higher than the activity of cells that grow as white colonies. Cells with the latter phenotype showed virtually no activity above background. In all cases the alkaline phosphatase activity increased when the same cells where grown overnight and assayed again. Except for SA72 (white) and SA308 (blue) the difference between the blue and white phenotypes

was still 1 order of magnitude.

Cells expressing fusion proteins resulting in a blue phenotype on XP plates and harvested in the exponential growth phase result in two major bands after Western blotting corresponding to the fusion proteins and mature PhoA (Fig. 5, *A* and *B*, *odd numbered lanes*). The relative mobilities of the upper bands decrease according to the increasing size of the N-terminal CitS fragments in the fusion proteins. Growth to the stationary phase results in the complete loss of the full-length fusion proteins, together with a marked increase of mature PhoA for the constructs shown in Fig. 5*A* (*even numbered lanes*). Apparently, the fusion proteins are unstable under these conditions, resulting in an accumulation of free PhoA in the periplasm. This behavior was observed for all constructs resulting in a blue phenotype, except for the two most N-terminal fusion proteins, SA46 and SA103, and the C-terminal fusion protein SA445, for which the full-length fusion protein could still be detected in the stationary phase (Fig. 5*B*). The general increase of the overall expression observed in the stationary phase is in line with the increased alkaline phosphatase activity (Table III). Cells expressing fusion proteins that appear as white colonies on XP plates behave quite differently. Representative examples are shown in Fig. 5*C*. The intensities of the bands are much lower, but in all cases a full-length fusion protein was observed with the cells from the exponential cultures showing synthesis of the proteins. The bands corresponding to mature PhoA were either absent or weak (*lanes 1*, *3*, and *5*). As observed with cells from the blue colonies, the full-length fusion proteins disappeared when the cells were grown to the stationary phase, but this was not accompanied by a significant increase of free PhoA (*lanes 2*, *4*, and *6*). Apparently, the PhoA part of the fusion protein is degraded rapidly when it is released into the cytoplasm. The more N-terminal fusions are present at higher intensities, but also more low molecular weight degradation products are visible (Fig. 5*D*). Full-length fusion protein SA72 is even present in the stationary growth phase together with a relatively high amount of
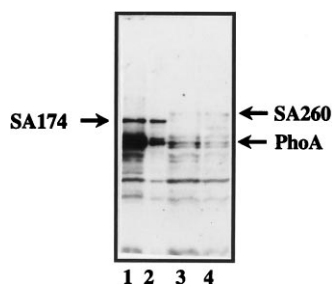
FIG. 6. **Cellular localization of free PhoA in cells with a white and blue phenotype.** Cells (*lanes 1* and *3*) expressing fusion proteins SA174 (blue; *lanes 1* and *2*) and SA260 (white; *lanes 3* and *4*) and spheroplasts derived from these cells (*lanes 2* and *4*) were analyzed for alkaline phosphatase by Western blotting as described in the legend to Fig. 5. The full-length fusion proteins and mature PhoA are indicated by *arrows*.

FIG. 7. **New secondary structure model of CitS.** CitS-PhoA fusions with high and low alkaline phosphatase activity are indicated by *filled* and *open circles*, respectively.

mature PhoA (*lane 2*), which may explain the somewhat higher PhoA activity relative to the cells from the other white colonies.

The cellular localization of the free PhoA part of the fusion proteins in cells with a blue and white phenotype is demonstrated in Fig. 6 for two representative examples. Spheroplasts were prepared from cells expressing fusion proteins SA174 (blue) and SA260 (white). Preparation of spheroplasts results in the release of periplasmic proteins. Immunoblot analysis showed that the spheroplasts of cells expressing SA174 had lost almost all of the PhoA, while the full-length fusion protein was present at the same intensity. In contrast, no difference in intensities was observed between the cells and spheroplasts with fusion SA260. Immunoblot analysis of cells from the exponential and stationary growth phases provides an independent assay of the cellular location of the PhoA moiety fused to N-terminal fragments of CitS.

A New Membrane Topology Model—The activity of the CitS-PhoA fusions proteins and the immunodetection analysis of the expressed proteins results in the localization of the fusion points as indicated in Table III. The cytoplasmic location of the N terminus and the localization of the first five fusion points (SA46, SA72, SA103, SA141, and SA174) conform to the model in Fig. 1 that was predicted from the primary sequence. The periplasmic localization of the two fusion sites flanking helix VI (SA174 and SA200) indicates that the entire domain between residues 174 and 200 is located in the periplasm and does not span the membrane. As a consequence, the orientation of the next TMSs in the membrane reverses, which is consistent with the localization of fusion sites 239, 260, and 290 for predicted TMSs VII and VIII. The seven active fusions at fusions points 290–360 indicate that this whole stretch is periplasmic and that the prediction of TMSs IX and X is falsified by the CitS-PhoA fusions. Fusions SA360 (blue) and SA379 (white) localize predicted TMS XI but in the opposite orientation. Finally, the cytoplasmic localization of fusion sites 389, 399, and 427 together with the periplasmic localization of the C terminus shows that predicted TMS XII is outgoing. The new model for the folding of CitS in the membrane based upon the results presented in this study is depicted in Fig. 7.

DISCUSSION

CitS forms together with the CitPs and MleP the family of the bacterial 2-hydroxycarboxylate transporters. The hydropathy profiles of the primary sequence of the three transporters are very similar, suggesting that their global structure is the same (13).[1] Secondary structure models predicted from the hydropathy profiles show 12 TMSs (Fig. 1 for CitS), which seems to be a general structural motif for bacterial secondary transporters. For many membrane proteins, the predicted secondary structure is supported by biochemical evidence or even
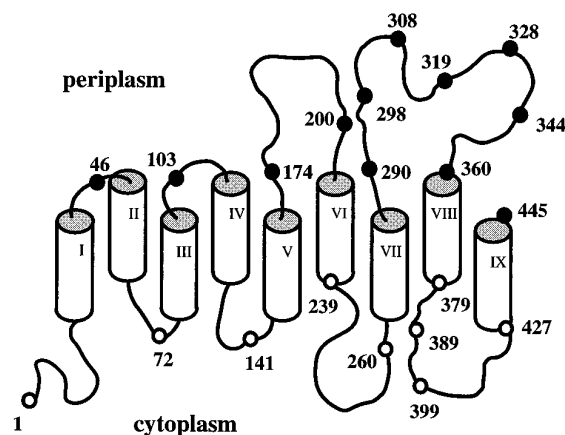
crystallographic data. The data presented in this paper are not consistent with the predicted model for CitS. The location of the N and C termini was determined by proteolysis experiments with CitS tagged at the N and C termini with a BAD, SB1 and SB445, respectively. Fusion of the BAD to the two termini leaves CitS active, indicating that the tags report on the native structure of the transporter (Table II). The BAD in SB1 was only accessible from the cytoplasmic side of the membrane, while the BAD in SB445 was only accessible from the periplasmic side, demonstrating that the N and C termini of CitS are located in the cytoplasm and periplasm, respectively (Fig. 4). Subsequently, a number of CitS-PhoA fusions were constructed to determine the number of times the polypeptide chain traverses the membrane. In a first approach, the fusion sites were selected in the hydrophilic regions flanking the predicted TMSs (Fig. 1, *lower arrows*). Detailed studies with the lactose permease, LacY, and the melibiose permease, MelB, of *E. coli* have indicated that half of an outgoing TMS is enough to export the PhoA part of a fusion protein to the periplasm and that half of an ingoing TMS is enough to prevent export (17, 30, 31). Therefore, the fusion sites in the hydrophilic stretches should report the localization correctly as long as they are not part of a TMS. Additional sites were selected especially in the C-terminal half of the protein to make sure that the polypeptide chain could not traverse the membrane in a helical conformation twice between two fusion points (Fig. 1, *upper arrows*). The results of these studies are that CitS traverses the membrane nine times with a cytoplasmic N terminus and a periplasmic C terminus.

The observation that about half of an outgoing TMS of a membrane protein is enough to export PhoA and that about half of an ingoing TMS is enough to prevent export means that the distance between two fusion points with the same high (or low) PhoA activity that are separated by a membrane-crossing segment may be as small as 25–30 residues (17). Therefore, two sites at this distance with the same phenotype may be in one continuous loop or halfway across the membrane in two adjacent TMSs. The latter would increase the number of times the protein traverses the membrane by two. We have inspected this possibility for the regions around the predicted TMSs that were falsified by the PhoA studies. The distance between the sites in SA174 and SA200 flanking predicted segment VI (Fig. 1) is 26 residues and both fusions have a blue phenotype. Positioning of the two sites halfway across the membrane would predict TMSs ranging approximately from residue 166 to 186 and from residue 186 to 206. The mean hydrophobicity of the latter stretch of residues is 0.07, which makes it highly unlikely that

this is a TMS. Therefore, we conclude that sites 174 and 200 are part of one periplasmic loop. The high alkaline phosphatase activity of the fusions at the hydrophilic sites 290, 328, and 360 that are separated by predicted TMSs IX and X (see Fig. 1) prompted us to investigate this region in more detail. Fusions were constructed at 10–15 residue spacings between positions 290 and 360. All of these constructs conferred high PhoA activity and showed the behavior in the immunoblot analysis that is typical for exported PhoA (Fig. 5). Fusion SA260 and the additional fusions at positions 379 and 389 set the length of the periplasmic loop to about 70 residues.

The low PhoA activity phenotype of cells expressing mature PhoA fused to N-terminal fragments of a membrane protein at cytoplasmic sites may be caused by low specific activity or by low levels of expression of the fusion protein. In the first mechanism, PhoA accumulates in the cytoplasm in an inactive form and can be detected by Western blotting (30). In the second mechanism, cytoplasmic PhoA is unstable and rapidly degraded, and it is not, or is poorly, detected by Western blotting (17, 31–33). Although both mechanisms are observed in different studies, it is not clear why a particular mechanism occurs. The CitS-PhoA fusions behave according to the second mechanism. Cells expressing CitS-PhoA fusion proteins were analyzed in the exponential growth phase and in the stationary phase, where proteolytic activity is usually higher. Full-length fusion proteins are observed for most of the constructs in the exponential growth phase, showing that the proteins are synthesized (Fig. 5). However, the level of expression of the high PhoA activity fusions is much higher than observed for the low activity fusions, indicating rapid degradation of the latter. Higher proteolytic activity in the stationary growth phase results in the degradation of the CitS fragment, and in the case of the high activity fusions it results in the accumulation of PhoA (Fig. 5*A*). The high PhoA activity observed in the stationary phase indicates that this fraction is active (Table III). Furthermore, preparation of spheroplasts from cells expressing high activity fusions results in the release of PhoA, showing its periplasmic localization (Fig. 6). Apparently, active PhoA in the periplasm is not very susceptible to proteolysis. In contrast, in the case of low activity fusions, PhoA does not accumulate in the stationary growth phase (Fig. 5*C*), and spheroplast preparation does not result in the release of the protein showing its cytoplasmic localization. In conclusion, inactive PhoA in the cytoplasm is more rapidly degraded than active PhoA in the periplasm. Remarkably, full-length fusion proteins are still observed in the stationary phase for the three most N-terminal fusions (SA46, SA72, and SA103) and for the C-terminal fusion, SA445 (Fig. 5, *B* and *D*). The higher stability of these fusion proteins may be due to a higher stability of these particular CitS fragments, which is the most reasonable explanation for the C-terminal fusion in which CitS assumes its native conformation (Table II).

The use of alkaline phosphatase as a periplasmic reporter enzyme is advantageous, in principle, because a positive result, *i.e.* a high activity fusion, requires the active export of the mature reporter enzyme moiety into the periplasm. In contrast, the use of β-galactosidase as a complementary cytoplasmic reporter may give a positive phenotype as a result of many artefacts (34). We have constructed 13 different CitS-LacZ fusions at fusion sites that result in high and in low activity CitS-PhoA fusions. Expression of the fusion proteins in different strains of *E. coli* and under different levels of induction never resulted in a significant difference in β-galactosidase activity of cells. As a rule, the cells expressing the different fusion proteins were either inactive or equally active in β-galactosidase activity. No further attempts were made to use the CitS-LacZ fusions for the topological studies.

The BAD of the oxaloacetate decarboxylase of *K. pneumoniae* was first used as a topological marker for membrane proteins in a study of the lactose permease of *E. coli* (35). It was shown that insertion of the BAD in periplasmic loops of LacY did not result in translocation of the domain across the membrane. Here we show that when BAD is fused to the C terminus of CitS the domain is translocated and ends up in the periplasm. In agreement with this observation, fusion of BAD to the C terminus of excreted proteins results in export of the domain (36). The periplasmic location of the BAD fused to the C terminus of CitS may explain the low amount of biotin detected in the Western blot analysis (Fig. 3). The similar citrate uptake activities of the N- and C-terminal fusions suggest that the level of expression of the fusion proteins is not very different. Therefore, the difference must be in the degree of biotinylation of the proteins. Biotinylation is a post-translational process that is catalyzed by biotin ligase in the cytoplasm. The low incorporation in the C-terminal fusion may be due to competition between biotinylation and export to the periplasm of the BAD. Recently, similar observations were made with the biotin acceptor domain of the transcarboxylase of *Propionibacterium shermanii* fused to the inner membrane protein MalF (37).

The new topology model of CitS based on the data presented in this paper represents a new structural class of secondary transporters. The structural motif consists of nine transmembrane segments and two large extramembrane domains at each side of the membrane in the C-terminal half of the protein (Fig. 7). The two cytoplasmic loops (residues 233–267 and 380–425) are hydrophilic. The latter, most C-terminal loop is well conserved in the 2-hydroxycarboxylate transporter family with 19 identical and 10 similar residues. The periplasmic loop between residues 170 and 210 is moderately hydrophobic and contains a glycine-rich stretch of 18 residues that is the most conserved region in the family. The second periplasmic domain of 70 residues (290–360) is remarkable, since it consists of two hydrophobic halves separated by a hydrophilic stretch of about 10 residues. Potentially, the hydrophobic regions of the two periplasmic loops fold between the transmembrane segments without completely crossing the membrane, as is believed to be the case for the voltage-gated potassium channels, where such structures are believed to form the translocation pore (38).

REFERENCES

1. Dimroth, P., and Thomer, A. (1986) *Biol. Chem. Hoppe Seyler* **367,** 813–823
2. Schwarz, E., and Oesterhelt, D. (1985) *EMBO J.* **4,** 1599–1603
3. van der Rest, M. E., Siewe, R. M., Abee, T., Schwarz, E., Oesterhelt, D., and Konings, W. N. (1992) *J. Biol. Chem.* **267,** 8971–8976
4. van der Rest, M. E., Molenaar, D., and Konings, W. N. (1992) *J. Bacteriol.* **174,** 4892–4898
5. Lolkema, J. S., Enequist, H., and van der Rest, M. E. (1994) *Eur. J. Biochem.* **220,** 469–475
6. Pos, M. K., Both, M., and Dimroth, P. (1995) *FEBS Lett.* **374,** 37–41
7. Pos, M. K., Dimroth, P. (1996) *Biochemistry* **35,** 1018–1026
8. David, S., van der Rest, M. E., Driessen, A. J. M., Simons, G., and de Vos, W. M. (1990) *J. Bacteriol.* **172,** 5789–5794
9. Vaughan, E. E., David, S., Harrington, A., Daly, C., Fitzgerald, G. F., and de Vos, W. M. (1995) *Appl. Environ. Microbiol.* **61,** 3172–3176
10. Eisenberg, D., Schwarz, E., Komarony, M., and Wall, R. (1984) *J. Mol. Biol.* **179,** 125–142
11. Poolman, B., Molenaar, D., Smid, E. J., Ubbink, T., Abee, T., Renault, P. P., and Konings, W. N. (1991) *J. Bacteriol.* **173,** 6030–6037
12. Marty-Teysset, C., Posthuma, C., Lolkema, J. S., Schmitt, P., Divies, C., and Konings, W. N. (1996) *J. Bacteriol.* **178,** 2178–2185
13. Lolkema, J. S., Konings, W. N., and Poolman, B. (1996) in *The Handbook of Biological Physics* (Konings, W. N., Kaback, H. R. and Lolkema, J. S., eds) Vol. II, pp. 229–260, Elsevier, Amsterdam
14. Marger, M. D., and Saier, Jr., M. H. (1993) *Trends Biochem. Sci.* **18,** 13–20
15. Von Heyne, G. (1986) *EMBO J.* **5,** 3021–3027
16. Kaback, H. R., Jung, K., Jung, H., Wu, J. and Privé, G. G. (1993) *J. Bioenerg. Biomembr.* **25,** 625–635
17. Pourcher, T., Bibi, E., Kaback, H. R., and Leblanc, G. (1996) *Biochemistry* **35,**

4161–4168
18. Poolman, B., and Konings, W. N. (1993) *Biochim. Biophys. Acta* **1183,** 5–39
19. Lolkema, J. S., Speelmans, G., and Konings, W. N. (1994) *Biochim. Biophys. Acta* **1187,** 211–215
20. Manoil, C., and Beckwith, J. (1986) *Science* **233,** 1403–1408
21. Sambrook, J., Fritsch, E. F., and Maniatis, T. (1989) *Molecular Cloning: A Laboratory Manual*, Cold Spring Harbor Laboratory Press, Cold Spring Harbor, NY
22. Studier, F. W., and Moffat, B. A. (1986) *J. Mol. Biol.* **189,** 113–130
23. Kunkel, T., Roberts, J. D., and Zakour, R. A. (1987) *Methods Enzymol.* **154,** 367–386
24. Sanger, F., Nicklen, S., and Coulson, A. R. (1977) *Proc. Natl. Acad. Sci. U. S. A.* **74,** 5463–5467
25. Consler, T. G., Persson, B. L., Jung, H., Zen, K. H., Jung, K., Privé, G. G., Kerner, G. E., and Kaback, H. R. (1993) *Proc. Natl. Acad. Sci. U. S. A.* **90,** 6934–6938
26. Gutierrez, C., and Devedjian, J. C. (1989) *Nucleic Acids Res.* **17,** 3999
27. Michaelis, S., Inouye, H., Oliver, D., and Beckwith, J. (1983) *J. Bacteriol.* **154,** 366–374
28. Kaback, H. R. (1971) *Methods Enzymol.* **22,** 99–120
29. Herzlinger, D., Viitanen, P., Carrasco, N., and Kaback, H. R. (1984) *Biochemistry* **23,** 3688–3693
30. Calamia, J., and Manoil, C. (1990) *Proc. Natl. Acad. Sci. U. S. A.* **87,** 4937–4941
31. Ujwal, M. L., Jung, H., Bibi, E., Manoil, C., Altenbach, C., Hubbell, W. L., and Kaback, H. R. (1995) *Biochemistry* **34,** 14909–14917
32. Gött, P., and Boos, W. (1988) *Mol. Microbiol.* **2,** 655–663
33. Lloyd, A. D., and Kadner, R. J. (1990) *J. Bacteriol.* **172,** 1688–1693
34. Yun, C. H., Van Doren, S. R., Crofts, A. R., and Gennis, R. B. (1991) *J. Biol. Chem.* **266,** 10967–10973
35. Zen, K. H., Consler, T. G., and Kaback, H. R. (1995) *Biochemistry* **34,** 3430–3437
36. Reed, K. E., and Cronan, J. E., Jr. (1991) *J. Biol. Chem.* **266,** 11425–11428
37. Jander, G., Cronan J. E., Jr., and Beckwith, J. (1996) *J. Bacteriol.* **178,** 3049–3058
38. Pongs, O. (1993) *J. Membr. Biol.* **136,** 1–8